Two-component millicharged dark matter and the EDGES 21 cm signal*

Qiaodan Li(黎乔丹)[1] Zuowei Liu(刘佐伟)[1,2†]

[1]Department of Physics, Nanjing University, Nanjing 210093, China
[2]Center for Excellence in Particle Physics, Chinese Academy of Sciences, Beijing 100049, China

Abstract: We propose a two-component dark matter explanation to the EDGES 21 cm anomalous signal. The heavier dark matter component is long-lived, and its decay is primarily responsible for the relic abundance of the lighter dark matter, which is millicharged. To evade the constraints from CMB, underground dark matter direct detection, and XQC experiments, the lifetime of the heavier dark matter has to be larger than $0.1\,\tau_U$, where τ_U is the age of the universe. Our model provides a viable realization of the millicharged dark matter model to explain the EDGES 21 cm signal, since the minimal model in which the relic density is generated via thermal freeze-out has been ruled out by various constraints.

Keywords: dark matter, 21 cm, new physics beyond the standard model

DOI: 10.1088/1674-1137/ac3d2b

I. INTRODUCTION

The hyperfine transition of the cosmic hydrogen atom, which is known as the 21 cm signal, provides a powerful probe to the physics in the early universe; for reviews, see Refs. [1-3]. Recently, the Experiment to Detect the Global Epoch of Reionization Signature (EDGES) has reported a new measurement on the sky-averaged radio spectrum centered at $\nu = 78$ MHz, which corresponds to the 21 cm absorption signal of the primordial hydrogen gas at redshift $z \simeq 17$ [4]. The differential brightness temperature T_{21} measured by the EDGES experiment at redshift $z \simeq 17$ is [4]

$$T_{21} = -500^{+200}_{-500}\ \text{mK}, \tag{1}$$

which is about a factor of two larger than the value expected in the standard cosmology [4, 5]. This hints that either the cosmic microwave background (CMB) could be hotter than expected [6-9], or the hydrogen gas could be colder than expected [10-27].

If the EDGES measurement is interpreted as caused by a colder gas, the question is how to cool the hydrogen gas? One simple solution is that, if there exist some sort of particle interactions between dark matter (DM) and hydrogen atom, the primordial hydrogen gas can be cooled by DM, which is colder than gas.[1)] However, there exist very strong constraints from the CMB measurements, as well as from other early universe measurements on DM interactions with standard model particles. Millicharged DM is one of the leading DM candidates to explain the EDGES anomaly, because its interaction with baryons is proportional to v^{-4}, where v is the relative velocity, thus leading to a much smaller interaction cross section in the early universe than that needed at $z \simeq 17$ for the EDGES interpretation so that the early universe constraints can be significantly alleviated. Millicharged DM has been extensively investigated for the interpretation of the EDGES anomaly [10-15, 19-22]. The parameter space of the millicharged DM is constrained by various experiments, including accelerator experiments [28], the CMB anisotropy [19, 20, 29-31], the SN1987A [32], and the Big Bang Nucleosynthesis (BBN) [12, 33, 34]; the allowed parameter space is that the millicharged DM mass is 0.1 MeV $\lesssim m_\chi \lesssim 10$ MeV, the millicharge is $10^{-6} \lesssim Q/e \lesssim 10^{-4}$, and the mass fraction of the millicharged DM is $0.0115\% \lesssim f \lesssim 0.4\%$. However, as pointed out by Ref. [21], such a parameter space is ruled out by the $N_{\rm eff}$ limit with the Planck 2018 data if the relic abundance of the millicharged DM is set by thermal freeze-out. Recently, Ref. [22] proposed a new millicharged DM model in which the sub-component millicharged DM has a sizable

Received 1 November 2021; Accepted 25 November 2021; Published online 21 February 2022

* Supported in part by the National Natural Science Foundation of China (11775109)

† E-mail: zuoweiliu@nju.edu.cn

1) A strong DM-baryon interaction can provide too much cooling such that T_{21} is even smaller the EDGES data. Thus, the EDGES measurement can also be used to constrian DM-baryon interactions.

interaction cross section with the other DM components so that the millicharged DM can be cooled by the other DM components; this reopens the parameter space that was previously excluded by various experimental constraints.

In this paper, we propose a new DM model that consists of two DM components: the lighter DM component is the millicharged DM, and the heavier DM component is unstable, which decays into the lighter DM component. In our model, the millicharged DM is primarily produced after the recombination, so that the stringent constraints from CMB can be alleviated. We show that such a model can explain the 21 cm anomaly observed by EDGES and satisfy various experimental constraints. The rest of the paper is organized as follows. We present our model in Sec. II. We compute the number density of the two DM components as a function of redshift in Sec. III. The temperature change due to the heavier DM decays is derived in Sec. IV. We provide the time evolution equations for four different physics quantities in Sec. V. The results of our numerical analysis are given in Sec. VI. We summarize our findings in Sec. VII.

II. THE MODEL

We extend the standard model (SM) by introducing a hidden sector that consists of three $U(1)$ gauge bosons, X^i_μ $(i=1,2,3)$, and one Dirac fermion χ that is charged under both X^2_μ and X^3_μ gauge bosons. We use the Stueckelberg mechanism [35-40] to provide mass to the three $U(1)$ gauge bosons; the new Lagrangian is given by

$$\begin{aligned}\Delta\mathcal{L} =& -\sum_{i=1,2,3}\frac{1}{4}X_{i\mu\nu}X_i^{\mu\nu}+\bar{\chi}(\mathrm{i}\gamma^\mu\partial_\mu-m_\chi)\chi\\ &+g_2^\chi X_2^\mu\bar{\chi}\gamma^\mu\chi+g_3^\chi X_3^\mu\bar{\chi}\gamma^\mu\chi\\ &-\frac{1}{2}(\partial_\mu\sigma_1+m_1'X_1^\mu)^2-\frac{1}{2}(\partial_\mu\sigma_2+m_1X_1^\mu+m_2X_2^\mu)^2\\ &-\frac{1}{2}(\partial_\mu\sigma_3+m_3X_3^\mu+m_4B^\mu)^2,\end{aligned}\tag{2}$$

where σ_1, σ_2, and σ_3 are the axion fields in the Stueckelberg mechanism, B_μ is the SM hypercharge boson, m_χ is the dark fermion mass, g_2^χ and g_3^χ are the gauge couplings, and m_1', m_1, m_2, m_3, and m_4 are the Stueckelberg mass terms. The Stueckelberg mechanism can be commonly seen in extra dimension models, strings, and D branes [41]. The Stueckelberg mechanism can also be viewed as a particular limit of the abelian Higgs mechanism, in which the Higgs mass goes to infinity and the Higgs vacuum expectation value is kept to be fixed [42]. However, unlike in the Higgs mechanism, mass is generated below the spontaneous symmetry breaking temperature in the early universe, in the Stueckelberg mechanism the vector boson can retain a mass to an arbitrary high temperature [43].

After the spontaneous symmetry breaking in the SM, the mass matrix M^2 of the neutral gauge bosons in the basis (X_1,X_2,X_3,B,A^3), where A^3 is the third component of the $SU(2)_\mathrm{L}$ gauge bosons in the SM, is given by

$$\begin{Bmatrix} m_1'^2+m_1^2 & m_1m_2 & 0 & 0 & 0\\ m_1m_2 & m_2^2 & 0 & 0 & 0\\ 0 & 0 & m_3^2 & m_3m_4 & 0\\ 0 & 0 & m_3m_4 & m_4^2+g_\mathrm{Y}^2v^2/4 & -g_\mathrm{Y}g_2v^2/4\\ 0 & 0 & 0 & -g_\mathrm{Y}g_2v^2/4 & g_2^2v^2/4 \end{Bmatrix},\tag{3}$$

where v is the vacuum expectation value of the SM Higgs, and g_2 and g_Y are the $SU(2)_\mathrm{L}$ and $U(1)_\mathrm{Y}$ gauge couplings in the SM respectively. The mass matrix has a vanishing determinant such that there exists a massless mode to be identified as the SM photon. Because the mass matrix is block-diagonal, one can diagonalize the first two gauge bosons and the last three gauge bosons separately.

The mass matrix of the first two gauge bosons (the upper-left two by two block matrix in Eq. (3)) can be diagonalized via a rotation matrix $\mathcal{R}$ which is parameterized by a single angle θ

$$\mathcal{R}=\begin{pmatrix}\cos\theta & -\sin\theta\\ \sin\theta & \cos\theta\end{pmatrix}.\tag{4}$$

The mass eigenstates, Z_1 and Z_2, are related to the gauge states via $Z_i=\mathcal{R}_{ji}X_j$. The rotation matrix $\mathcal{R}$ leads to an interaction between χ and Z_1 such that $\mathcal{L}_\mathrm{int}=\sin\theta g_2^\chi Z_1^\mu\bar{\chi}\gamma^\mu\chi\equiv v_{Z_1}^\chi Z_1^\mu\bar{\chi}\gamma^\mu\chi$. We are interested in the parameter space where $\theta\ll1$ so that $Z_1\sim X_1$ and $Z_2\sim X_2$. In our analysis, we take $m_1'\sim2m_\chi$, $m_2<m_\chi$, and $m_1\ll m_2$ so that the two mass eigenstates have masses $m_{Z_1}\simeq m_1'$ and $m_{Z_2}\simeq m_2$, and the mixing angle θ is given by $\theta\simeq m_1m_2/(m_1'^2-m_2^2)$.

The mass matrix of the last three gauge bosons (the bottom-right three by three block matrix in Eq. (3)) can be diagonalized by an orthogonal matrix O such that $E_i=O_{ji}G_j$, where $G_j=(X_3,B,A^3)$ are the gauge states, and $E_i=(Z',Z,\gamma)$ are the mass eigenstates. Here, γ is the photon, Z is the neutral gauge boson in the weak interaction, and Z' is the new massive vector boson. Thus, we have $O^TM^2_{3\times3}O=\mathrm{diag}(m^2_{Z'},m^2_Z,0)$, where $M^2_{3\times3}$ is the bottom-right three by three block matrix in Eq. (3). Such a matrix diagonalization also leads to interactions between matter fields (both hidden sector fermion χ and SM fermions f) and the three mass eigenstates (γ, Z, and Z'). The interaction Lagrangian can be parameterized as follows

$$\bar{f}\gamma_\mu(v_i^f-\gamma_5 a_i^f)fE_i^\mu+v_i^\chi\bar{\chi}\gamma_\mu\chi E_i^\mu, \tag{5}$$

where the vector and axial-vector couplings are given by

$$v_i^f=(g_2O_{3i}-g_YO_{2i})T_f^3/2+g_YO_{2i}Q_f, \tag{6}$$

$$a_i^f=(g_2O_{3i}-g_YO_{2i})T_f^3/2, \tag{7}$$

$$v_i^\chi=g_\chi O_{1i}. \tag{8}$$

Here, Q_f is the electric charge of the SM fermion, and T_f^3 is the quantum number of the left-hand chiral component under $SU(2)_{\rm L}$.

Thus, the hidden sector fermion χ has a vector current interaction with the SM photon,

$$v_3^\chi A_\mu\bar{\chi}\gamma^\mu\chi\equiv\epsilon eA_\mu\bar{\chi}\gamma^\mu\chi, \tag{9}$$

where we have defined an electric charge ϵ for the χ particle. In our analysis, we adopt the following model parameters: $m_3=100$ TeV, and $m_4/m_3\ll1$. In this case, the electric charge ϵ is given by $\epsilon\simeq-(m_4/m_3)\cos\theta_W(g_3^\chi/e)$, where θ_W is the weak rotation angle in the SM. Since $m_4/m_3\ll1$ in our analysis, we have $\epsilon\ll1$, which is often referred to as millicharge. χ is then the millicharged particle.

III. TWO DM COMPONENTS

There are two DM particles in the hidden sector, the Z_1 boson and the hidden Dirac fermion χ. In the very early universe, Z_1 is the dominant DM component, which is assumed to be nonthermally produced. The Z_1 DM component is long-lived and decays into $\bar{\chi}\chi$. The decay width of the Z_1 boson is given by

$$\begin{aligned}\Gamma(Z_1\to\bar{\chi}\chi)&=\frac{m_{Z_1}}{12\pi}\sqrt{1-4\frac{m_\chi^2}{m_{Z_1}^2}}\left(1+2\frac{m_\chi^2}{m_{Z_1}^2}\right)(v_{Z_1}^\chi)^2\\&\simeq\frac{\sqrt{m_{Z_1}\Delta m}}{4\sqrt{2}\pi}\left(g_2^\chi\theta\right)^2,\end{aligned} \tag{10}$$

where $v_{Z_1}^\chi=g_2^\chi\sin\theta\simeq g_2^\chi\theta$, $\Delta m\equiv m_{Z_1}-2m_\chi$, and we have assumed $\Delta m\ll m_{Z_1}$. In our analysis, we have $\theta\ll1$ and $\Delta m\ll m_{Z_1}$ so that Z_1 is long-lived with a lifetime

$$\tau(Z_1)\simeq\sqrt{\frac{\rm MeV}{m_{Z_1}}}\sqrt{\frac{\rm meV}{\Delta m}}\left(\frac{2.3\times10^{-16}}{g_2^\chi\theta}\right)^2\tau_{17}, \tag{11}$$

where $\tau_{17}\sim7\times10^{15}$ second is the time between the early universe and $z=17$.

The value of Δm cannot be very large, otherwise the DM χ will be significantly heated by the decay process $Z_1\to\bar{\chi}\chi$ so that χ is unable to cool the baryons. The velocity of the χ particle is $v_\chi\simeq\sqrt{\Delta m/m_\chi}$ in the rest frame of Z_1, under the assumption of $\Delta m\ll m_\chi$. For the case where $m_\chi\sim100$ MeV and $\Delta m\sim O$(meV), we have $v_\chi\sim3.2\times10^{-6}$. Thus, in our analysis, we assume a sufficiently small mass difference, $\Delta m\sim O$(meV), such that the Z_1 decay does not heat the χ DM significantly.

The χ DM component is mainly produced via the decay process $Z_1\to\bar{\chi}\chi$ in the universe. We assume that the initial number density of χ is negligible. The relic density of χ can also be produced via thermal freeze-out. There are two processes that contribute to the χ DM annihilation cross section: $\bar{\chi}\chi\to\gamma\to\bar{f}f$ and $\bar{\chi}\chi\to Z_2Z_2$. In our analysis, $\sigma(\bar{\chi}\chi\to Z_2Z_2)\gg\sigma(\bar{\chi}\chi\to\bar{f}f)$. The $\bar{\chi}\chi$ annihilation cross section into on-shell Z_2 bosons is given by [44]

$$\langle\sigma v\rangle(\bar{\chi}\chi\to Z_2Z_2)\simeq\frac{(g_2^\chi)^4}{16\pi m_\chi^2}\frac{(1-r^2)^{3/2}}{(1-r^2/2)^2}, \tag{12}$$

where $r=m_{Z_2}/m_\chi$. For the case where $g_2^\chi=1$, $r=1/2$, and $m_\chi=5$ MeV, one has $\langle\sigma v\rangle(\bar{\chi}\chi\to Z_2Z_2)\simeq0.3$ barn, leading to a mass fraction as $f_\chi\sim10^{-11}$. Thus, the contribution to the relic density of χ from thermal freeze-out is negligible, and the constraints imposed on thermal freeze-out millicharged DM (e.g. Ref. [21]) are not directly applicable to our model.

The total number of Z_1 particles in a comoving volume at time t is given by

$$N_{Z_1}(t)=N_{Z_1}(0)\mathrm{e}^{-t/\tau}, \tag{13}$$

where τ is the lifetime of the Z_1 particle, $N_{Z_1}(0)$ is the total number of Z_1 particles at time $t=0$, and we have assumed that Z_1 is non-relativistic. In our analysis, we set $t=0$ at redshift $z_0=10^6$; the abundance of Z_1 at $z_0=10^6$ is given by $\rho_{Z_1}(z_0)\simeq\rho_{\rm DM,0}(1+z_0)^3$, where $\rho_{\rm DM,0}$ is the current DM density. The number of χ particles at time t in a comoving volume is $N_\chi(t)=2N_{Z_1}(0)-2N_{Z_1}(t)$. Thus, the number density of χ is related to the number density of Z_1 via

$$n_\chi=2(\mathrm{e}^{t/\tau}-1)n_{Z_1}. \tag{14}$$

where n_{Z_1} (n_χ) is the number density of the Z_1 (χ) particle. In our analysis $m_{Z_1}\simeq2m_\chi$, so the mass fraction of the millicharged DM χ at redshift z in the total DM is given by

$$f_\chi(z)\simeq(1-\mathrm{e}^{-t(z)/\tau}), \tag{15}$$

where $t(z)$ is the time between early universe (which we take to be $z_0 = 10^6$) and redshift z[1]. Fig. 1 shows the mass fraction of χ as a function of the redshift z for different lifetimes τ. CMB observations provide strong constraints on millicharged DM; only 0.4% DM can be millicharged, unless the millicharge is negligible [19, 20, 31]. This leads to a lower bound on the τ, which is $\sim 3.6\times10^{15}$ s.

Because $\Delta m \ll m_\chi$, the total DM density $\rho_{Z_1}+\rho_\chi$ at redshift z is given by $\rho_{Z_1}+\rho_\chi = \rho_{\rm DM,0}(1+z)^3$. Thus, the number density of χ particles at redshift z is given by

$$n_\chi(z) = \frac{\rho_{\rm DM,0}}{m_\chi}(1+z)^3 f_\chi(z) \simeq \frac{\rho_{\rm DM,0}}{m_\chi}(1+z)^3(1-{\rm e}^{-t(z)/\tau}), \quad (16)$$

where $\rho_{\rm DM,0} = \Omega_{\rm DM}\rho_{\rm cr,0}$ and $\rho_{\rm cr,0} = 1.054h^2\times10^4$ eV cm^{-3} is the critical density [45]. In our analysis, we use $\Omega_{\rm DM}h^2 = 0.1186$ [46].

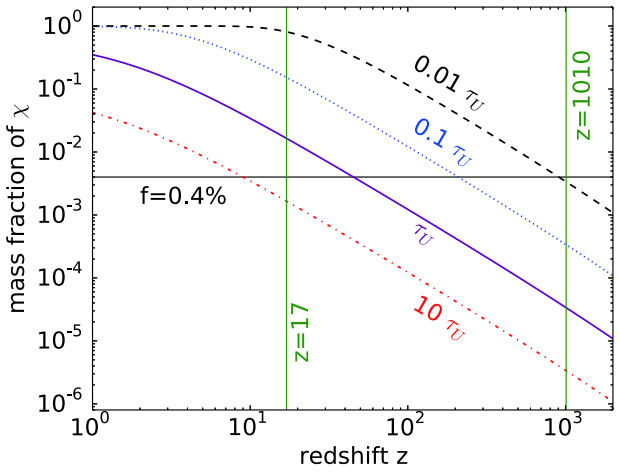

Fig. 1. (color online) Mass fraction of χ in the total DM as a function of the redshift. $\tau_U \simeq 4.3\times10^{17}$ s is the age of the universe.

IV. DM TEMPERATURE INCREASE GENERATED BY DECAYS

The DM χ is heated by the $Z_1 \to \chi\bar{\chi}$ decay process because of the difference between the Z_1 mass and twice of the χ mass. To compute this effect, consider the kinetic energy Δq that goes into the $\chi\bar{\chi}$ final state for the decay process $Z_1 \to \chi\chi$

$$\Delta q = \Delta m + \frac{3}{2}k_{\rm B}T_{Z_1}, \quad (17)$$

where $3k_{\rm B}T_{Z_1}/2$ is the averaged kinetic energy of Z_1 with T_{Z_1} being the temperature of the Z_1 particle and $k_{\rm B}$ being the Boltzmann constant[2]. Here, we have assumed that Z_1 is non-relativistic and Δm is sufficiently small, such that χ is also non-relativistic. The change in the particle numbers in the comoving volume per unit time due to decay is given by $\dot{N}_{Z_1} = -\Gamma_{Z_1}N_{Z_1}$ and $\dot{N}_\chi = -2\dot{N}_{Z_1}$, where the dot denotes the derivative with respect to time, N_χ (N_{Z_1}) is the particle number of χ (Z_1), and Γ_{Z_1} is the decay width for the process $Z_1 \to \chi\chi$. The total kinetic energy transfer to the χ particles per unit time from Z_1 decays is given by $\Delta q|\dot{N}_{Z_1}|$, which is equal to the change of the kinetic energy of the χ particles per unit time

$$\Delta q|\dot{N}_{Z_1}| = \frac{\rm d}{{\rm d}t}\left(\frac{3}{2}k_{\rm B}T_\chi N_\chi\right) = \frac{3}{2}k_{\rm B}(T_\chi\dot{N}_\chi + N_\chi\dot{T}_\chi). \quad (18)$$

Thus, the χ temperature change per unit time due to Z_1 decays is given by

$$\dot{T}_\chi^d = \frac{n_{Z_1}}{n_\chi}\left[\frac{2}{3k_{\rm B}}\Delta m + T_{Z_1} - 2T_\chi\right]\Gamma_{Z_1}. \quad (19)$$

V. TIME EVOLUTION EQUATIONS

To compute the baryon temperature at redshift $z = 17$, we numerically solve the temperature evolutions for various quantities.

The time evolution equation of the baryon temperature T_b is given by (see e.g. [10, 47])

$$\frac{{\rm d}T_b}{{\rm d}t} = -2HT_b + \frac{2}{3}\frac{{\rm d}Q_b}{{\rm d}t} + \Gamma_C(T_\gamma - T_b), \quad (20)$$

where H is the Hubble parameter[3], T_γ is the CMB temperature, Q_b is the energy transfer term due to DM-baryon scatterings, and $\Gamma_{\rm C}$ is the Compton scattering rate which describes the effects due to CMB-baryon interactions. The Compton scattering rate is given by [10]

$$\Gamma_{\rm C} = \frac{8\sigma_{\rm T}x_e}{3(1+f_{\rm He})m_e}U \quad (21)$$

where $\sigma_{\rm T}$ is the Thomson cross section, $f_{\rm He}$ is the Helium fraction, and U is the energy density. In our analysis, we use $\sigma_{\rm T} = 6.65\times10^{-25}$ cm^2 [45], $f_{\rm He} = 0.08$ [10], and $U = (\pi^2/15)T_\gamma^4 = 0.26(1+z)^4$ eV/cm^3 [48, 49].

The time evolution equation of the temperature T_χ of

1) The formulas to compute $t(z)$ are given in Appendix A.

2) For a system without thermal equilibrium, T_{Z_1} represents the average kinetic energy of Z_1. This treatment is acceptable since EDGES only measures the sky-averaged brightness temperature.

3) See Appendix A for the calculation of H.

the lighter DM component χ is given by

$$\frac{\mathrm{d}T_\chi}{\mathrm{d}t} = -2HT_\chi + \frac{2}{3}\frac{\mathrm{d}Q_\chi}{\mathrm{d}t} + \dot{T}^d_\chi, \tag{22}$$

where Q_χ is the energy transfer term due the interaction between DM χ and baryons, and $\dot{T}^d_\chi$ is given in Eq. (19). The first two terms on the right-hand side of Eq. (22) represent the effects due to universe expansion and the DM-baryon scattering respectively, which are similar to the first two terms in Eq. (20). The third term on the right-hand side of Eq. (22) is new and is due to the decay of the Z_1 particle in our model, as discussed in Sec. IV.

In addition, we also solve the time evolution equation of the relative bulk velocity between baryon and DM, $V_{\chi b} = |\vec{V}_{\chi b}|$ where $\vec{V}_{\chi b} \equiv \vec{V}_\chi - \vec{V}_b$ [47],

$$\frac{\mathrm{d}V_{\chi b}}{\mathrm{d}t} = -HV_{\chi b} - D(V_{\chi b}), \tag{23}$$

and the time evolution equation of the ionization fraction $x_e \equiv n_e/n_H$ [50]

$$\frac{\mathrm{d}x_e}{\mathrm{d}t} = -C\left[n_H\alpha_B {x_e}^2 - 4(1-x_e)\beta_B \exp\left(\frac{3E_0}{4T_\gamma}\right)\right]. \tag{24}$$

We follow Ref. [50] to obtain the various coefficients in Eq. (24). The formulas of Q_b, Q_χ, and $D(V_{\chi b})$ for millicharged DM used in our analysis are given in Appendix B.

VI. RESULTS

We simultaneously solve the four time evolution equations for T_b, T_χ, $V_{\chi b}$, and x_e from redshift $z = 1010$ to $z = 10$. The baryon temperature T_b at $z = 1010$ is assumed to be equal to the CMB temperature $T_\gamma = T_0(1+z)$,where $T_0 = 2.7$ K, since these two components are tightly coupled in the early universe. The temperatures for both DM components are assumed to be negligible in the early universe, so we set $T_{Z_1} = 0$ and $T_\chi = 0$ at $z = 1010$. This is due to the fact that in our model, Z_1 does not interact with the SM particles and $\Delta m \ll m_\chi$. We also set $x_e = 0.05$ [51] and $V_{\chi b} = 29$ km/s [10] at redshift $z = 1010$.

We scan the parameter space spanned by ϵ and m_χ for three different decay lifetimes of Z_1: $\tau = 2\times10^{16}$, 3×10^{17}, and 8×10^{17} s. In our analysis, we fix $\Delta m = 1$ meV. In order to explain the EDGES data, the baryon temperature T_b has to be at least 5.1 K at $z = 17$ within the 99% CL [22]. Fig. 2 shows the parameter space where the baryon temperature can be cooled to $T_b = 5.1$ K at $z = 17$ for three different lifetimes of Z_1: 2×10^{16} (blue dot-dashed), 3×10^{17} (purple dashed), and 8×10^{17} s (red solid)[1)]. Millicharged DM is mainly constrained by CMB around $z \simeq 10^3$ [61]. The mass fractions of χ at $z = 1100$ are about 0.06%, 0.004%, and 0.001% for the lifetimes $\tau = 2\times10^{16}$, 3×10^{17}, and 8×10^{17} s, respectively, which satisfy the CMB bound $f_\chi < 0.4\%$ [20]. However, in our model, the mass fraction of the millicharged DM increases with redshift. Energy injections after the recombination can further influence the CMB power spectrum and thus, are constrained by the CMB data (see Refs. [62-66]). Thus, we compute the mass fractions of χ at $z = 600$, which are about 0.15%, 0.01%, and 0.004% for the lifetimes $\tau = 2\times10^{16}$, 3×10^{17}, and 8×10^{17} s, respectively. Because the mass fractions for all the models con-

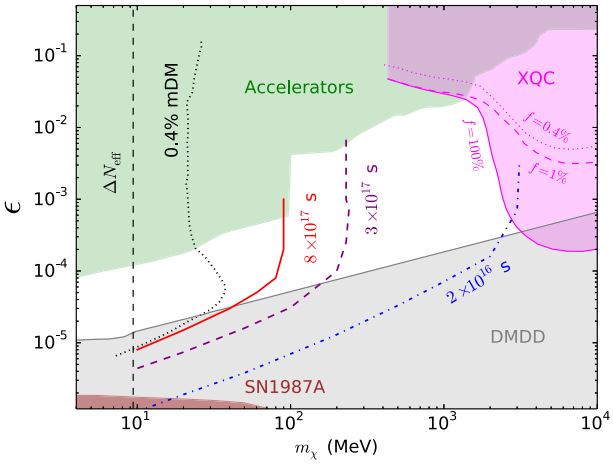

Fig. 2. (color online) Parameter space spanned by the millicharge ϵ and the DM mass m_χ. Model points in which $T_b = 5$ K at $z = 17$ correspond to three different lifetimes: $\tau = 2\times10^{16}$ s (blue dot-dashed), $\tau = 3\times10^{17}$ s (purple dashed), and $\tau = 8\times10^{17}$ s (red solid), with the mass fraction of the millicharged DM component being 0.06%, 0.004%, and 0.001% at $z = 1100$, and 100%, 77%, and 42% today, respectively. The green shaded region is excluded by various accelerator experiments, including SLAC electron beam dump [28], CMS [52], MiniBooNE and LSND [53], ArgoNeuT [54], milliQan demonstrator [55], and others [56, 57]. The gray shaded region indicates the parameter region excluded by the dark matter direct detection (DMDD) experiments; above the DMDD region, millicharged DM is absorbed by the rocks on top of underground labs [22, 58]. The magenta region is ruled out by the rocket experiment XQC for mass fractions: $f = 100\%$ (solid) [59], $f = 1\%$ (solid) [59], and $f = 0.4\%$ (solid) [58]. The brown shaded region is excluded by the SN1987A data [60]. The black dashed vertical line indicates the upper bound on DM mass due to $\Delta N_{\rm eff}$ from CMB [12, 33]. The black dotted line indicates the parameter space of the minimal millicharged DM model with a mass fraction of 0.4% to explain EDGES data [22].

1) We note that the three curves will move towards the right direction if the magnitude of T_{21} becomes smaller.

Table 1. Benchmark model points. All the masses are in unit of MeV. We take $g_2^\chi = g_3^\chi = 1$ in our analysis.

Model	m_1'	m_1	m_2	m_3	m_4	m_χ	Δm	θ	ϵ	τ_{Z_1}/s
A	160	10^{-13}	1.55	10^8	2.76×10^3	~80	10^{-9}	6.1×10^{-18}	8×10^{-5}	8×10^{17}
B	400	10^{-8}	1.25×10^{-4}	10^8	3.45×10^3	~200	10^{-9}	7.8×10^{-18}	1×10^{-4}	3×10^{17}

sidered in this analysis are smaller than 0.4% for redshift $z > 600$, the CMB constraints are satisfied [20][1]. We find that the viable parameter in our model is much larger than the minimal millicharged DM model[2], which is indicated by the black dotted line for 0.4% millicharged DM [22]. Various experimental constraints are considered in Fig. 2. These include, the underground dark matter direct detection (DMDD) experiments [22, 58], the XQC experiment [58, 59], SN1987A [60], and the accelerator experiments: SLAC electron beam dump [28], CMS [52], MiniBooNE [53], LSND [53], ArgoNeuT [54], and milliQan demonstrator [55]. Two benchmark model points that can explain the 21 cm anomaly while satisfying various constraints are presented in Table 1. The mass fractions of the χ DM at today are 100%, 77%, and 42% for the lifetimes $\tau = 2\times10^{16}$, 3×10^{17}, and 8×10^{17} s, respectively. We find that the Z_1 lifetime 2×10^{16} is nearly excluded by both the underground DMDD and the XQC constraints. In order to evade the XQC constraints, the Z_1 lifetime has to be $\geqslant 2\times10^{16}$ s.

VII. CONCLUSIONS

We construct a new millicharged DM model to explain the recent 21 cm anomaly. In our model, the millicharged DM χ is a subcomponent in the early universe and is mainly produced via decays of the other DM component Z_1. The DM annihilation cross section $\bar{\chi}\chi \to Z_2Z_2$ is so strong that the relic abundance of χ due to thermal freeze-out is negligible. We compute the heating term due to the decay process $Z_1 \to \bar{\chi}\chi$ and include it in our numerical calculations of the time evolution equation of the DM temperature. We find that the model can explain the EDGES 21 cm anomaly while satisfying various experimental constraints, including those from accelerators, XQC, underground DMDD, and CMB.

ACKNOWLEDGEMENT

We thank Ran Ding and Mingxuan Du for helpful discussions.

APPENDIX A: TIME

The time $t(z)$ at redshift z is given by

$$t(z) = \int_z^{z_0} \frac{\mathrm{d}z'}{H(z')(1+z')}, \tag{A1}$$

where H is the Hubble parameter. Here, we use $z_0 = 10^6$. We compute the Hubble parameter at redshift z via

$$H(z) = H_0\sqrt{\Omega_R(1+z)^4 + \Omega_m(1+z)^3 + \Omega_\Lambda}, \tag{A2}$$

where $H_0 \equiv 100h\ \mathrm{km\ s^{-1}\ Mpc^{-1}}$ is the present Hubble parameter, Ω_R, Ω_m, and Ω_Λ are the density of radiation, matter, and dark energy, respectively. In our analysis, we adopt the following values: $\Omega_R = 2.47\times10^{-5}/h^2$ [67], $\Omega_m = 0.308$, $\Omega_\Lambda = 0.692$, and $h = 0.678$ [46].

APPENDIX B: MILLICHARGED DM FORMULAS

We provide the formulas of $\sigma_{0,t}$, Q_b, Q_χ, and $D(V_{\chi b})$ for millicharged DM used in our analysis.

The scattering cross section between millicharged DM and baryons can be parameterized as $\sigma_t = \sigma_{0,t}v^{-4}$ where v is the relative velocity between DM and baryons, and $\sigma_{0,t} = 2\pi\alpha^2\epsilon^2\xi/\mu_{\chi t}^2$ where α is the fine structure constant, ϵ is the millicharge, $\mu_{\chi t}$ is the reduced mass of DM χ and the target particle t, and ξ is the Debye logarithm [10, 68] $\xi = \ln\left[9T_b^3/(4\pi\epsilon^2\alpha^3 x_e n_H)\right]$.

The baryon heating term due to interactions with millicharged DM is given by [10, 47]

$$\frac{\mathrm{d}Q_b}{\mathrm{d}t} = n_\chi x_e \sum_{t=e,p} \frac{m_t m_\chi}{(m_\chi+m_t)^2}\frac{\sigma_{0,t}}{u_{\mathrm{th},t}} \times\left[\sqrt{\frac{2}{\pi}}\frac{\mathrm{e}^{-r_t^2/2}}{u_{\mathrm{th},t}^2}(T_\chi - T_b) + m_\chi\frac{F(r_t)}{r_t}\right], \tag{B1}$$

where $u_{\mathrm{th}}^2 \equiv T_b/m_b + T_\chi/m_\chi$, $r \equiv V_{\chi b}/u_{\mathrm{th}}$, and $F(r) = \mathrm{erf}\left(r/\sqrt{2}\right) - \sqrt{2\pi}r\mathrm{e}^{-r^2/2}$. Here, we assume that electron and proton share a common temperature T_b with the hydrogen atom. The DM heating term due to interactions with baryons is given by

$$\frac{\mathrm{d}Q_\chi}{\mathrm{d}t} = n_H x_e \sum_{t=e,p} \frac{m_\chi m_t}{(m_\chi+m_t)^2}\frac{\sigma_{0,t}}{u_{\mathrm{th},t}}$$

1) We note that, because χ in our model is smaller at larger redshift, the allowed mass fraction of χ at $z \simeq 600$ should be somewhat larger than 0.4%, which is obtained assuming a constant mass fraction. A detailed analysis taking into account the variation of the mass fraction is beyond the scope of this study.

2) In the minimal millicharged DM model, the millicharge interaction is responsible for both DM thermal freeze-out and cooling the cosmic hydrogen atoms.

$$\times\left[\sqrt{\frac{2}{\pi}}\frac{\mathrm{e}^{-r_i^2/2}}{u_{\mathrm{th},t}^2}(T_b-T_\chi)+m_t\frac{F(r_t)}{r_t}\right], \tag{B2}$$

where $n_e=n_p=n_H x_e$ is assumed.

The D term in Eq. (23) is given by [47]

$$D(V_{\chi b})=\frac{\rho_m\sigma_0}{m_\chi+m_b}\frac{F(r)}{V_{\chi b}^2}, \tag{B3}$$

where we consider both electron and proton as the target baryons.

References

[1] S. Furlanetto, S. P. Oh, and F. Briggs, Phys. Rept. **433**, 181-301 (2006), arXiv:astroph/0608032[astro-ph]
[2] M. F. Morales and J. S. B. Wyithe, Ann. Rev. Astron. Astrophys. **48**, 127-171 (2010), arXiv:0910.3010[astroph.CO]
[3] J. R. Pritchard and A. Loeb, Rept. Prog. Phys. **75**, 086901 (2012), arXiv:1109.6012[astroph.CO]
[4] J. D. Bowman, A. E. E. Rogers, R. A. Monsalve *et al.*, Nature **555**(7694), 67-70 (2018), arXiv:1810.05912[astro-ph.CO]
[5] A. Cohen, A. Fialkov, R. Barkana *et al.*, Mon. Not. Roy. Astron. Soc. **472**(2), 1915-1931 (2017), arXiv:1609.02312[astro-ph.CO]
[6] C. Feng and G. Holder, Astrophys. J. Lett. **858**(2), L17 (2018), arXiv:1802.07432[astro-ph.CO]
[7] S. Fraser, A. Hektor, G. Hütsi *et al.*, Phys. Lett. B **785**, 159-164 (2018), arXiv:1803.03245[hep-ph]
[8] T. Moroi, K. Nakayama, and Y. Tang, Phys. Lett. B **783**, 301-305 (2018), arXiv:1804.10378[hep-ph]
[9] E. D. Kovetz, I. Cholis, and D. E. Kaplan, Phys. Rev. D **99**(12), 123511 (2019), arXiv:1809.01139[astro-ph.CO]
[10] J. B. Muñoz and A. Loeb, Nature **557**(7707), 684 (2018), arXiv:1802.10094[astro-ph.CO]
[11] A. Fialkov, R. Barkana, and A. Cohen, Phys. Rev. Lett. **121**, 011101 (2018), arXiv:1802.10577[astro-ph.CO]
[12] A. Berlin, D. Hooper, G. Krnjaic *et al.*, Phys. Rev. Lett. **121**(1), 011102 (2018), arXiv:1803.02804[hep-ph]
[13] R. Barkana, N. J. Outmezguine, D. Redigolo *et al.*, Phys. Rev. D **98**(10), 103005 (2018), arXiv:1803.03091[hep-ph]
[14] R. Barkana, Nature **555**(7694), 71-74 (2018), arXiv:1803.06698[astroph.CO]
[15] T. R. Slatyer and C. Wu, Phys. Rev. D **98**(2), 023013 (2018), arXiv:1803.09734[astro-ph.CO]
[16] L. B. Jia, Eur. Phys. J. C **79**(1), 80 (2019), arXiv:1804.07934[hep-ph]
[17] N. Houston, C. Li, T. Li *et al.*, Phys. Rev. Lett. **121**(11), 111301 (2018), arXiv:1805.04426[hep-ph]
[18] P. Sikivie, Phys. Dark Univ. **24**, 100289 (2019), arXiv:1805.05577[astro-ph.CO]
[19] E. D. Kovetz, V. Poulin, V. Gluscevic *et al.*, Phys. Rev. D **98**(10), 103529 (2018), arXiv:1807.11482[astro-ph.CO]
[20] K. K. Boddy, V. Gluscevic, V. Poulin *et al.*, Phys. Rev. D **98**(12), 123506 (2018), arXiv:1808.00001[astro-ph.CO]
[21] C. Creque-Sarbinowski, L. Ji, E. D. Kovetz *et al.*, Phys. Rev. D **100**(2), 023528 (2019), arXiv:1903.09154[astro-ph.CO]
[22] H. Liu, N. J. Outmezguine, D. Redigolo *et al.*, Phys. Rev. D **100**(12), 123011 (2019), arXiv:1908.06986[hep-ph]
[23] A. Aboubrahim, P. Nath, and Z. Y. Wang, *EDGES data as a signal of the Stueckelberg mechanism in the early universe*, arXiv: 2108.05819[hep-ph]
[24] S. Clark, B. Dutta, Y. Gao *et al.*, Phys. Rev. D **98**(4), 043006 (2018), arXiv:1803.09390[astro-ph.HE]
[25] K. Cheung, J. L. Kuo, K. W. Ng *et al.*, Phys. Lett. B **789**, 137-144 (2019), arXiv:1803.09398[astro-ph.CO]
[26] C. Li and Y. F. Cai, Phys. Lett. B **788**, 70-75 (2019), arXiv:1804.04816[astro-ph.CO]
[27] A. Halder, M. Pandey, D. Majumdar *et al.*, JCAP **10**, 033 (2021), arXiv:2105.14356[astro-ph.CO]
[28] A. A. Prinz, R. Baggs, J. Ballam *et al.*, Phys. Rev. Lett. **81**, 1175-1178 (1998), arXiv:hep-ex/9804008[hep-ex]
[29] S. Dubovsky, D. Gorbunov, and G. Rubtsov, JETP Lett. **79**, 1-5 (2004), arXiv:hepph/0311189[hep-ph]
[30] A. Dolgov, S. Dubovsky, G. Rubtsov *et al.*, Phys. Rev. D **88**(11), 117701 (2013), arXiv:1310.2376[hep-ph]
[31] R. de Putter, O. Dor, J. Gleyzes *et al.*, Phys. Rev. Lett. **122**(4), 041301 (2019), arXiv:1805.11616[astro-ph.CO]
[32] J. H. Chang, R. Essig, and S. D. McDermott, JHEP **09**, 051 (2018), arXiv:1803.00993[hepph]
[33] C. Boehm, M. J. Dolan, and C. McCabe, JCAP **08**, 041 (2013), arXiv:1303.6270[hep-ph]
[34] P. F. Depta, M. Hufnagel, K. Schmidt-Hoberg *et al.*, JCAP **04**, 029 (2019), arXiv:1901.06944[hep-ph]
[35] B. Kors and P. Nath, JHEP **07**, 069 (2005), arXiv:hep-ph/0503208[hep-ph]
[36] D. Feldman, Z. Liu, and P. Nath, Phys. Rev. Lett. **97**, 021801 (2006), arXiv:hep-ph/0603039[hep-ph]
[37] D. Feldman, Z. Liu, and P. Nath, JHEP **11**, 007 (2006), arXiv:hep-ph/0606294[hep-ph]
[38] D. Feldman, Z. Liu, and P. Nath, Phys. Rev. D **75**, 115001 (2007), arXiv:hep-ph/0702123[hep-ph]
[39] D. Feldman, Z. Liu, P. Nath *et al.*, Phys. Rev. D **80**, 075001 (2009), arXiv:0907.5392[hep-ph]
[40] M. Du, Z. Liu, and V. Tran, JHEP **05**, 055 (2020), arXiv:1912.00422[hep-ph]
[41] P. Nath, Mod. Phys. Lett. A **25**, 3003-3016 (2010), arXiv:0812.0958[hep-ph]
[42] T. J. Allen, M. J. Bowick, and A. Lahiri, Mod. Phys. Lett. A **6**, 559-572 (1991)
[43] A. E. Nelson and J. Scholtz, Phys. Rev. D **84**, 103501 (2011), arXiv:1105.2812[hep-ph]
[44] J. M. Cline, G. Dupuis, Z. Liu *et al.*, JHEP **08**, 131 (2014), arXiv:1405.7691[hep-ph]
[45] E. W. Kolb and M. S. Turner, Front. Phys. **69**, 1-547 (1990)
[46] P. Ade *et al.*, Astron. Astrophys. **594**, A13 (2016), arXiv:1502.01589[astro-ph.CO]
[47] J. B. Muñoz, E. D. Kovetz, and Y. Ali-Haïmoud, Phys. Rev. D **92**(8), 083528 (2015), arXiv:1509.00029[astro-ph.CO]
[48] S. Seager, D. D. Sasselov, and D. Scott, Astrophys. J. Suppl. **128**, 407-430 (2000), arXiv:astro-ph/9912182[astro-ph]
[49] P. J. E. Peebles, Principles of physical cosmology
[50] Y. Ali-Haimoud and C. M. Hirata, Phys. Rev. D **83**, 043513 (2011), arXiv:1011.3758[astro-ph.CO]
[51] S. S. McGaugh, Phys. Rev. Lett. **121**(8), 081305 (2018), arXiv:1808.02532[astro-ph.CO]

[52] S. Chatrchyan *et al*., Phys. Rev. D **87**(9), 092008 (2013), arXiv:1210.2311[hepex]
[53] G. Magill, R. Plestid, M. Pospelov *et al*., Phys. Rev. Lett. **122**(7), 071801 (2019), arXiv:1806.03310[hepph]
[54] R. Acciarri *et al*., Phys. Rev. Lett. **124**(13), 131801 (2020), arXiv:1911.07996[hep-ex]
[55] A. Ball, G. Beauregard, J. Brooke *et al*., Phys. Rev. D **102**(3), 032002 (2020), arXiv:2005.06518[hep-ex]
[56] S. Davidson, S. Hannestad, and G. Raffelt, JHEP **05**, 003 (2000), arXiv:hep-ph/0001179[hep-ph]
[57] A. Badertscher, P. Crivelli, W. Fetscher *et al*., Phys. Rev. D **75**, 032004 (2007), arXiv:hep-ex/0609059[hep-ex]
[58] T. Emken, R. Essig, C. Kouvaris *et al*., JCAP **09**, 070 (2019), arXiv:1905.06348[hep-ph]
[59] M. S. Mahdawi and G. R. Farrar, JCAP **10**, 007 (2018), arXiv:1804.03073[hep-ph]
[60] M. Fabbrichesi, E. Gabrielli, and G. Lanfranchi, *The Dark Photon*, arXiv: 2005.01515[hep-ph]
[61] W. L. Xu, C. Dvorkin, and A. Chael, Phys. Rev. D **97**(10), 103530 (2018), arXiv:1802.06788[astro-ph.CO]
[62] T. R. Slatyer, N. Padmanabhan, and D. P. Finkbeiner, Phys. Rev. D **80**, 043526 (2009), arXiv:0906.1197[astro-ph.CO]
[63] T. R. Slatyer, Phys. Rev. D **87**(12), 123513 (2013), arXiv:1211.0283[astro-ph.CO]
[64] N. Aghanim *et al*. (Planck), *Planck 2018 results. VI. Cosmological parameters*, Astron. Astrophys. A **641**, 6 (2020) [Erratum: Astron. Astrophys. C **652**, 4 (2021)], arXiv: 1807.06209[astro-ph.CO]
[65] M. Kawasaki, K. Nakayama, and T. Sekiguchi, Phys. Lett. B **756**, 212-215 (2016), arXiv:1512.08015[astro-ph.CO]
[66] W. C. Huang, J. L. Kuo, and Y. L. S. Tsai, JCAP **06**, 025 (2021), arXiv:2101.10360[astro-ph.CO]
[67] S. Dodelson, Modern Cosmology
[68] S. D. McDermott, H. Yu, and K. M. Zurek, Phys. Rev. D **83**, 063509 (2011), arXiv:1011.2907[hep-ph]